HAL
open science

# Error thresholds for self- and cross-specific enzymatic replication

Benedikt Obermayer, Erwin Frey

## To cite this version:

Benedikt Obermayer, Erwin Frey. Error thresholds for self- and cross-specific enzymatic replication. Journal of Theoretical Biology, 2010, 267 (4), pp.653. 10.1016/j.jtbi.2010.09.016 . hal-00637810

**HAL Id: hal-00637810**

**https://hal.science/hal-00637810v1**

Submitted on 3 Nov 2011

**HAL** is a multi-disciplinary open access archive for the deposit and dissemination of scientific research documents, whether they are published or not. The documents may come from teaching and research institutions in France or abroad, or from public or private research centers.

L'archive ouverte pluridisciplinaire **HAL**, est destinée au dépôt et à la diffusion de documents scientifiques de niveau recherche, publiés ou non, émanant des établissements d'enseignement et de recherche français ou étrangers, des laboratoires publics ou privés.

Author's Accepted Manuscript

www.elsevier.com/locate/yjtbi

# Error thresholds for self- and cross-specific enzymatic replication

Benedikt Obermayer, Erwin Frey

PII: S0022-5193(10)00490-X
DOI: doi:10.1016/j.jtbi.2010.09.016
Reference: YJTBI 6156

To appear in: *Journal of Theoretical Biology*

Received date: 5 March 2010
Revised date: 28 July 2010
Accepted date: 9 September 2010

Cite this article as: Benedikt Obermayer and Erwin Frey, Error thresholds for self- and cross-specific enzymatic replication, *Journal of Theoretical Biology*, doi:10.1016/j.jtbi.2010.09.016

This is a PDF file of an unedited manuscript that has been accepted for publication. As a service to our customers we are providing this early version of the manuscript. The manuscript will undergo copyediting, typesetting, and review of the resulting galley proof before it is published in its final citable form. Please note that during the production process errors may be discovered which could affect the content, and all legal disclaimers that apply to the journal pertain.

ACCEPTED MANUSCRIPT

# Error thresholds for self- and cross-specific enzymatic replication

Benedikt Obermayer[a], Erwin Frey[a,*]

[a] *Arnold-Sommerfeld-Center for Theoretical Physics and Center for NanoScience, Ludwig-Maximilians-Universität München, Theresienstr. 37, 80333 München, Germany*

**Abstract**

The information content of a non-enzymatic self-replicator is limited by Eigen's error threshold. Presumably, enzymatic replication can maintain higher complexity, but in a competitive environment such a replicator is faced with two problems related to its twofold role as enzyme and substrate: as enzyme, it should replicate itself rather than wastefully copy non-functional substrates, and as substrate it should preferably be replicated by superior enzymes instead of less-efficient mutants. Because specific recognition can enforce these propensities, we thoroughly analyze an idealized quasispecies model for enzymatic replication, with replication rates that are either a decreasing (self-specific) or increasing (cross-specific) function of the Hamming distance between the recognition or "tag" sequences of enzyme and substrate. We find that very weak self-specificity suffices to localize a population about a master sequence and thus to preserve its information, while simultaneous localization about complementary sequences in the cross-specific case is more challenging. A surprising result is that stronger specificity constraints allow longer recognition sequences, because the populations are better localized. Extrapolating from experimental data, we obtain rough quantitative estimates for the maximal length of the recognition or tag sequence that can be used to reliably discriminate appropriate and infeasible enzymes and substrates, respectively.

*Corresponding author

*Email addresses:* obermayer@physik.lmu.de (Benedikt Obermayer), frey@physik.lmu.de (Erwin Frey)



Accepted manuscript

ACCEPTED MANUSCRIPT

*Keywords:* origin of life, quasispecies theory, enzymatic self-replication, higher-order catalysis

## 1. Introduction

The acclaimed experimental finding (Cech, 1990) that RNA not only stores genetic information but also provides catalytic function has inspired the RNA world scenario (Gilbert, 1986), a hypothesis for the starting point of Darwinian evolution at the origin of life through self-replication of RNA-like polynucleotides. Substantial progress over the last decades demonstrates the capability of RNA enzymes (ribozymes) to catalyze diverse chemical reactions (Doudna and Cech, 2002; Lilley, 2005; Joyce, 2007), among them the polymerization of as many as 20 nucleotides to a template molecule (Johnston et al., 2001; Zaher and Unrau, 2007), and even replication through template-directed ligation reactions involving short RNA oligomers as building blocks (Lincoln and Joyce, 2009). However, the currently known systems are not yet capable of Darwinian evolution, lacking either the ability to replicate molecules as long and complex as themselves or to introduce heritable variation.

For theorists, the focus has mainly been on whether the information content of a self-replicating molecule can be maintained in the presence of replication errors, usually employing Eigen's well-known quasispecies theory (Eigen et al., 1989) for the self-replication of $L$-nucleotide sequences. In this model, replication errors occur with an error probability $\mu$ per single nucleotide, and the replication rates are taken as functions only of the template sequence. This mapping from genotype to replication rate (or fitness) presents a considerable challenge for evolutionary models, and even generic structural features of such fitness landscapes, such as the extent of ruggedness and epistasis, are under debate. Valuable insight comes from experiments on mutagenized ribozymes (Kun et al., 2005) and from computer simulations using RNA secondary structure as phenotype (Huynen et al., 1996; Takeuchi et al., 2005), which indicate a significant degree of neutrality around an optimal sequence, reducing the deleterious

Accepted manuscript

ACCEPTED MANUSCRIPT

effects of mutations. Other theoretical studies used a large number of different idealized fitness landscapes, e.g., with a single peak at one fittest "master" sequence (Swetina and Schuster, 1982; Leuthäusser, 1986; Schuster and Swetina, 1988; Woodcock and Higgs, 1996; Galluccio, 1997; Hermisson et al., 2002; Peliti, 2002; Saakian and Hu, 2006; Saakian et al., 2009), with some rather generic results (Wiehe, 1997; Jain and Krug, 2005): the population in sequence space is characterized by a broad mutant distribution (a quasispecies) localized about the master sequence for mutation probabilities smaller than a critical value $\mu_c$ (the error threshold), while it consists of random sequences (it is delocalized) for larger values. Because the error threshold $\mu_c \sim 1/L$ is usually inversely proportional to sequence length, the problem arises whether the maximally sustainable complexity of a self-replicator suffices to perform the complex task of self-replication (Eigen and Schuster, 1978).

In a prebiotic context, it is important to emphasize that using a fitness landscape where rates depend only on the template sequence pertains to non-enzymatic rather than enzymatic replication, because in the latter case the replication rates also depend on the concentrations and the characteristics of involved enzymes. For RNA, the potential for non-enzymatic replication is questionable, given that template-directed polymerization or ligation seems limited to short molecules with rather specific sequences (von Kiedrowski, 1986; Acevedo and Orgel, 1987; Wu and Orgel, 1992; Orgel, 2004). Moreover, experimental and simulation studies demonstrate a strongly disadvantageous tendency for elongating side-reactions at the cost of replication (Fernando et al., 2007). Hence, although there have been speculations (Pace and Marsh, 1985), it remains unclear how a single more complex RNA should literally copy itself (Joyce, 2007; Szostak et al., 2001).

Enzymatic replication is more plausible (Orgel, 1992), but raises the question whether high replication efficiency (high fitness) is a property of the substrate or the enzyme. In the latter case, a superior replicase does not enjoy a selective advantage, because it replicates non-functional mutant templates just as well as itself, while it is not guaranteed in the former case that a superior template is

Accepted manuscript

ACCEPTED MANUSCRIPT

functional at all. Likewise, mutations generate substrates that are replicated less efficiently, but they also produce less-efficient enzymes (Maynard Smith, 1979), thus affecting the replication rates of all potential substrates. On theoretical grounds, one should expect that a superior replicator is a good enzyme and a good substrate *at the same time*. As enzyme, it should therefore replicate only functional substrates, and as substrate, it should be replicated preferably by efficient enzymes. It has long been realized that in a competitive environment these propensities are crucial for the emergence, improvement and perpetuation of replicase activity, which is essentially an altruistic trait that is not by itself selected for (Michod, 1983). The commonly proposed solution to render enzymatic replication evolutionarily stable is to impose a form of group selection, e.g., via compartmentalization in vesicles, in order to keep similar molecules closely together (Szathmáry and Demeter, 1987; Alves et al., 2001; Fontanari et al., 2006), even though this requires a simultaneous and coordinated emergence of replicators and protocells (Szostak et al., 2001). However, known ribozymes act with moderately or even strongly substrate-specific efficiency (Joyce, 2007), such that *specific recognition* may also have a significant influence. Since unspecific reactions require sophisticated substrate-binding properties that could well have been a rather late invention in prebiotic evolution (Johnston et al., 2001), it seems natural to assume that replication efficiency should depend strongly on the interaction between enzyme and substrate.

In this paper, we analyze a general model of enzymatic replication accounting both for varying degrees of specificity and the characteristically broad quasispecies distributions in order to address the consequences for the error threshold. Similar to models for the evolution of regulatory DNA motifs (Gerland and Hwa, 2002), we assume that specificity depends on the quality of binding to some recognition or tag sites (Weiner and Maizels, 1987). Idealizing this condition, we use replication rates that depend on the Hamming distance between these sequence regions of enzyme and substrate via a decreasing (self-specific) or increasing (cross-specific) function. After formulating the model and discussing our analytical approach in a methods section, we show for these two scenarios

Accepted manuscript

ACCEPTED MANUSCRIPT

results from stochastic simulations and numerical solutions of deterministic rate equations. Using our analytical toolbox, we discuss the resulting localization conditions, error thresholds and the phase diagram. In our conclusions, we use experimental values for polymerization rates to obtain simple estimates for the maximum number of nucleotides that can be used for recognition.

## 2. Model

In the framework of quasispecies theory, each molecule is characterized by its sequence $S_i = (\sigma_1^{(i)} \dots \sigma_L^{(i)})$ of $L$ binary nucleotides $\sigma_\ell^{(i)} \in \{0, 1\}$. In an infinitely large population, its concentration $X_i$ evolves according to the deterministic rate equations (Eigen et al., 1989)

$$\dot{X}_i = \sum_j M_{ij} R_j X_j - X_i \sum_j R_j X_j. \tag{1}$$

Here, $M_{ij} = \mu^{d_{ij}}(1-\mu)^{L-d_{ij}}$ is the mutation probability between sequences $S_i$ and $S_j$ with Hamming distance $d_{ij} = \sum_\ell |\sigma_\ell^{(i)} - \sigma_\ell^{(j)}|$, where $\mu$ is the error probability per single nucleotide (usually called "mutation rate"), and the replication rate $R_i$ of sequence $S_i$ is given by:

$$R_i = A_i + \sum_j B_{ij} X_j. \tag{2}$$

Whereas the non-enzymatic rate $A_i$ depends only on the genotype $S_i$, the second term implies frequency-dependent selection and makes our model intrinsically nonlinear. It encodes the catalytic interactions of two molecules: $B_{ij}$ measures how well $S_j$ catalyzes the replication of $S_i$. The second term in Eq. (1) ensures the normalization $\sum_j X_j = 1$, and a degradation term $-D_i X_i$ therefore drops out of Eq. (1) since we assume that the decay rate $D_i \equiv D$ is sequence-independent for simplicity. Note that actual RNA sequences replicate via a complementary intermediate, while our idealized model assumes direct replication in a single step. It has been shown that these two approaches are essentially equivalent for the symmetric situations considered here (Stadler, 1991).

Accepted manuscript

ACCEPTED MANUSCRIPT

To capture the pertinent features of a situation where replicase enzymes prefer to replicate themselves instead of their competitors, we assume that the quality of specific recognition influences catalytic rates more strongly than the actual genotypes of enzyme and substrate. Hence, we effectively only model the recognition regions of ribozymes, which are often clearly separated from the catalytic domains (Lilley, 2005). Of course, the proper function of the latter region is indispensable, but in our idealized model we neglect the influence of mutations: as we have shown previously in a simple model, their effect on the error threshold is largely independent from the more interesting consequences of mutations in the recognition region (Obermayer and Frey, 2009). The sequence length $L$ is thus restricted to the number of nucleotides that take part in recognition. Probably mediated via specific base-pairing interactions (Doudna and Cech, 2002), the quality of recognition can be taken as function of the number of mismatches between the binding sites of enzyme and substrate, and we let the catalytic matrix $B_{ij}$ therefore depend via a *specificity function* $f(d)$ only on the Hamming distance $d_{ij}$ between enzyme and substrate. Further, because rate enhancements through ribozyme catalysis can be substantial (Doudna and Cech, 2002), such that non-enzymatic replication rates are comparably small (if nonzero at all), we neglect their genotype dependence altogether and choose a flat fitness landscape for $A_i$:

$$A_i \equiv \alpha, \qquad B_{ij} = \beta f(d_{ij}). \tag{3}$$

Because we are interested in the stationary state, the parameter $\alpha$ (if nonzero) merely sets the time scale while $\beta$ measures the selection strength.

We will first analyze a scenario for self-specific replication, where replication rates increase with *similarity* of enzyme and substrate. To have the degree of specificity explicitly tunable via a parameter $p$, we use the specificity function

$$f_{\mathrm{s}}(d) = (1 - d/L)^p. \tag{4}$$

As a contrasting example, we will then analyze a similarly defined specificity function where replication rates increase with *complementarity* between enzyme



Accepted manuscript

ACCEPTED MANUSCRIPT

and substrate:

$$f_c(d) = (d/L)^p. \tag{5}$$

The numerical and analytical approach presented in the next section can readily be applied to other functional forms of the specificity function.

## 3. Methods

For reasonably large sequence length, the full $2^L$-dimensional system Eq. (1) can only be analyzed using stochastic simulations in a finite population of $N$ sequences. Here, we employ the straightforward stochastic simulation algorithm used by Wilke et al. (2001). At time $t$ each sequence $S_k$, present in $N_k$ copies, has a probability $p_{0,k} = N_k / \sum_i N_i(1+R_i)$ to be copied without mutations into the population at time $t+1$, and a probability $p_{\mathrm{mut},jk} = M_{jk} R_k N_k / \sum_i N_i(1+R_i)$ to be selected and mutated into sequence $S_j$. Following initialization, our observables of interest are measured by averaging over time after reaching a stationary state.

In order to derive analytical results, we exploit that the stationary states of Eq. (1) are localized about a particular "master" sequence $S_*$, which is necessary to preserve its information content. In contrast, delocalization indicates that such a sequence $S_*$ cannot be maintained due to replication errors. Since the possibility of non-trivial dynamics such as periodic orbits cannot be excluded for general replicator-mutator equations like Eq. (1) (Stadler et al., 1995), there might also be other reasons for the absence of localization. However, we did not find any signs of complex dynamical behavior in our simulations, and one can easily convince oneself that the delocalized state, where all sequences have the same concentration and therefore identical replication rates, can lead to localization: since replication rates are essentially proportional to concentration, stochastic concentration fluctuations imply higher rates. Unless hindered by excessive mutations, this can induce a transition to a state localized about some randomly chosen master sequence, which then also has the highest replication rate (see Obermayer and Frey (2009) for a visualization). Such "fixation" events



Accepted manuscript

ACCEPTED MANUSCRIPT

are very similar to the phenomenon of consensus formation, e.g., in language dynamics (Blythe, 2009). Note that our idealized replication rates do not predetermine any specific master sequence for localization. This symmetry would be broken in a full model where replication rates depend on the full genotypes of enzyme and substrate (and not just the Hamming distance between their recognition regions).

Given localization about $S_*$, we can significantly reduce the dimensionality of Eq. (1) by lumping all sequences $S_i$ with a Hamming distance $k$ to $S_*$ together into "error class" $k$. Without loss of generality, we assume that $S_* = (00\ldots0)$. This well-known procedure (Schuster and Swetina, 1988; Woodcock and Higgs, 1996) permits to formulate reduced rate equations formally equivalent to Eq. (1) in terms of new variables $x_k$ denoting the concentration of error class $k$ in the population:

$$\dot{x}_k = \sum_{ji} m_{kj}[a_j\delta_{ji} + b_{ji}x_i]x_j - x_k \sum_{ji}[a_j\delta_{ji} + b_{ji}x_i]x_j. \tag{6}$$

Here and in the following, we use lowercase letters for all variables in the reduced system. For our model Eq. (3), the non-enzymatic rates are given by $a_i \equiv \alpha$. The accordingly reduced mutation matrix and the catalytic matrix depend only on the Hamming distance between pairs of sequences in different error classes (measured with respect to the master sequence), which allows us to combinatorially assess all possibilities for their relative distance. The total probability of distributing $0 \leq k - j + 2\ell \leq L$ mutations to move a sequence from error class $j$ into error class $k$ has been derived previously as (Woodcock and Higgs, 1996)

$$m_{kj} = \sum_{\ell} \binom{L-j}{k-j+\ell}\binom{j}{\ell}(1-\mu)^{L-(k-j+2\ell)}\mu^{k-j+2\ell}. \tag{7}$$

The replication rate Eq. (2) also depends on the frequency of each sequence in each error class. With the homogeneity assumption that all $\binom{L}{j}$ sequences in class $j$ are equally populated, this complication can be resolved, and the reduced



Accepted manuscript

ACCEPTED MANUSCRIPT

matrix $b_{ij}$ reads analogously

$$b_{ij} = \beta \sum_n \binom{L-i}{j-i+n} \binom{i}{n} \frac{f(j-i+2n)}{\binom{L}{j}}. \tag{8}$$

Numerical solutions to the $(L+1)$-dimensional rate equations given in Eq. (6) can now easily be found by means of standard algorithms.

A more detailed understanding of these solutions can be obtained from the population distribution's normalized first moment $a = \langle k \rangle / L = \langle \sigma \rangle$, which as the mean Hamming distance $\langle k \rangle = \sum_k k x_k$ to the master $S_* = (00\ldots0)$ characterizes the width of the distribution and measures the mean value $\langle \sigma \rangle$ of each sequence's binary nucleotides. Writing down an equation for the first moment of Eq. (6) requires a hierarchy of expressions for higher moments, which can be truncated by means of a moment closure technique. For the self-specific case, we assume that the stationary Hamming distance distribution is approximately binomial, $x_k \approx \binom{L}{k} a^k (1-a)^{L-k}$, because this reproduces the expected distribution in the limits $a \to 0$ (complete localization about one sequence) and $a \to 1/2$ (the delocalized state, where the binary nucleotides are random numbers). Moreover, it solves the rate equations Eq. (1) exactly for linear fitness landscapes without epistasis (Woodcock and Higgs, 1996) and for an extension of the quasispecies model to a game theory setting (Lässig et al., 2003). With this binomial ansatz, $a$ is the population distribution's only parameter, and for our model of the replication rates Eq. (3), it obeys the equation

$$(1-2a)\Big\{\mu L\left[\alpha + \beta S(1-2a(1-a))\right] - a(1-a)(1-2\mu)\beta S'(1-2a(1-a))\Big\} = 0. \tag{9}$$

This equation for $a$, which is one of our main analytical results (see Appendix A.1 for a derivation), holds for *any* specificity function $f(d)$, which enters via the function

$$S(x) = \sum_k \binom{L}{k} f(k)\, x^{L-k} (1-x)^k. \tag{10}$$

An intuitive interpretation of this auxiliary function derives from recognizing that the quantity $\alpha + \beta S(1-2a(1-a))$ measures the *mean replication rate* (or



Accepted manuscript

ACCEPTED MANUSCRIPT

mean fitness) $\sum_j R_j X_j$ of the population if $a$ solves Eq. (9). Such solutions $a(\mu)$ can be obtained explicitly only in special cases where $S(x)$ attains a simple form (see Appendix A.2), but we can easily solve for $\mu(a)$ and invert graphically to obtain a *bifurcation diagram*:

$$\mu(a) = \left[2 + \frac{\alpha + \beta S(1 - 2a(1-a))}{\beta a(1-a) S'(1 - 2a(1-a))}\right]^{-1}. \tag{11}$$

For cross-specific replication with the specificity function Eq. (5), we expect two equivalent subpopulations localized about complementary sequences, which corresponds to a superposition of binomial distributions: $x_k \approx \frac{1}{2}\binom{L}{k}\left[a^k(1-a)^{L-k} + (1-a)^k a^{L-k}\right]$. To obtain an equation similar to Eq. (9) for their mean widths $a$, we cannot use the first moment of the reduced rate equations (it vanishes by construction, because the distribution is symmetric about $a = 1/2$), but use the second moment $\left\langle \Delta k^2 \right\rangle = \sum_k (k - \langle k \rangle)^2 x_k$, leading to a lengthy result explicitly given in Appendix B.1 and a corresponding expression for the bifurcation diagram (see Eqs. (B.5) and (B.7)).

## 4. Results and Discussion

### *4.1. Self-specific replication*

Our first scenario is concerned with self-specific replication, where replication rates increase with similarity of enzyme and substrate through the specificity function Eq. (4). As argued in the preceding section, stochastic fluctuations increasing the frequency of one particular sequence also increase its replication rate, such that the population can localize about this master sequence $S_*$. Figure 1 shows the stationary Hamming distance distribution $x_k$, which measures the concentration of sequences with $k$ mutations relative to $S_*$, for different degrees of specificity from the linear case $p = 1$ to complete self-specificity $p \to \infty$, where enzyme and substrate have to be identical. We compare results from stochastic simulations to numerical solutions of the reduced rate equations, Eq. (6). The excellent agreement between simulation and deterministic

Accepted manuscript

ACCEPTED MANUSCRIPT

theory justifies the homogeneity assumption made in symmetrizing the specificity matrix (see Eq. (8)). In the simulations shown in Fig. 1, we initialized all sequences at a predetermined master sequence in order to avoid noise from the intrinsically stochastic "fixation" events, but we also tested other initial conditions with modest inhomogeneities, which were quickly "washed out" and did not give rise to measurable differences in the stationary state.

The limit $p \to \infty$ with $f_{\mathrm{s}}(d) \to \delta_{d,0}$, depicted in Fig. 1(c), leads to a generalized Schlögl model of auto-catalytic replication, which has been partly analyzed by Stadler et al. (1995). In this limit we can employ the well-known "error-tail" approximation (Schuster and Swetina, 1988): we define $x_0$ as the concentration of the master sequence, $\alpha + \beta x_0$ its replication rate and $(1-\mu)^L$ the probability not to have a mutation. All other sequences are lumped together in the error tail with concentration $1 - x_0$ and replication rate $\alpha$ (the concentration of suitable replicase enzymes is so small that the frequency-dependent term in the replication rate does not contribute). Neglecting back mutations from the error tail into $x_0$ (corresponding to the large-genome limit), we obtain the simple equation

$$\dot{x}_0 = (\alpha + \beta x_0)(1-\mu)^L x_0 - x_0 \bar{r}, \tag{12}$$

with $\bar{r} = (\alpha + \beta x_0)x_0 + \alpha(1 - x_0)$ the mean replication rate. In the stationary state, we easily find that the delocalized state $x_0 = 0$ is stable for all $\mu$, while a branch of solutions with nonzero $x_0$ emerges for $(1-\mu)^L > 2(\sqrt{\alpha(\alpha+\beta)} - \alpha)/\beta$ through a *discontinuous* transition (see also Campos et al. (2000); Obermayer and Frey (2009); Wagner et al. (2010) for similar results in related models). Whereas for the somewhat related sharply-peaked fitness landscape, where only the master sequence has a higher replication rate, the error threshold arises through a *continuous* bifurcation (Baake and Wiehe, 1997), the discontinuity observed here expresses the qualitatively different behavior we previously termed "escalation of error catastrophe" (Obermayer and Frey, 2009): as the mutation rate grows, the proportion of fittest sequences, i.e., of the necessary replicase enzymes, is diminished and therefore their replication rate. This in turn reduces



Accepted manuscript

ACCEPTED MANUSCRIPT

their concentration, until at the error threshold the concentration of enzymes $x_0$ is not large enough to have them replicate with an efficiency sufficient for localization.

Although Eq. (12) approximates the exact result for $x_0$ very well (see the dashed line in Fig. 1(c)), it is valid only for $L \to \infty$ (because back mutations are neglected) and $p \to \infty$ (because the replication rate of the error-tail is taken as concentration-independent). In order to gain a more general perspective, we use the analytical solutions of Eq. (9) for the mean Hamming distance to the master (the population distribution's first moment $a = \langle k \rangle / L$) obtained from the bifurcation diagram Eq. (11). A comparison between the exact solution $a(\mu)$ resulting from the reduced rate equations Eq. (6) via numerical continuation[1] and Eq. (11) is shown in Fig. 2 for $L = 8$, $\alpha = \beta = 1$ and different values of $p$ in the specificity function Eq. (4). Recalling the symmetry of the original model, Eq. (3), namely that the population can localize about any sequence, the remaining reflection symmetry $a \to 1 - a$ about the delocalized solution $a = 1/2$ indicates that after symmetrization localization is only possible about the master sequence or its complement. The stable branches associated with localized solutions start for $\mu = 0$ at $a = 0$ (or $a = 1$), i.e., full localization about one sequence (or its complement), and higher mutation rates give rise to broader distributions with larger mean, until these localized regimes disappear at critical mutation rates $\mu_c$ denoted by circles. The delocalized solutions, on the other hand, gain stability at finite mutation rates $\tilde{\mu}_c$ (denoted by crosses), and we find bistability for $\tilde{\mu}_c < \mu < \mu_c$. A similar situation is encountered in formally related models of grammar evolution (Nowak et al., 2001; Komarova, 2004).

Explicit expressions for the error threshold $\mu_c = \max \mu(a)$ are available from Eq. (11) when the auxiliary function $S(x)$ (defined in Eq. (10)) has a simple form (see Appendix A.2). For instance, $\mu_c = \beta/(4\alpha L + 2\beta(L+1))$ for $p = 1$, where specificity decreases linearly with the distance between enzyme and substrate.

[1] AUTO software package available via `http://indy.cs.concordia.ca/auto/`.



Accepted manuscript

ACCEPTED MANUSCRIPT

Although an error threshold is absent for linear fitness landscapes without epistasis (Woodcock and Higgs, 1996), here the intrinsically nonlinear model gives a sharp transition even in this apparently similar case. For very strong specificity $p \to \infty$ we find $\mu_\mathrm{c} = \mathcal{W}[\beta/(\mathrm{e}\alpha)]/(2L)$ using Lambert's $\mathcal{W}$-function, and we recover the result $\mu_\mathrm{c} = \ln(\beta/\alpha)/(2L)$ that can also be obtained from the error-tail approximation in the limit $\beta \gg \alpha$. Further, the delocalized state $a = 1/2$ is the only solution of Eq. (9) in the complete absence of specificity ($f_\mathrm{s}(d) \equiv 1$), supporting the intuition that unspecific replication does not suffice to preferentially maintain the information of one particular sequence. Interestingly, taking $p \to 0$ in Eq. (4) gives the finite even though exponentially small value $\mu_\mathrm{c} = \beta/(2^{L+1}(\alpha+\beta))$. This result implies that limited localization is possible even for very weak specificity (if $p = 0$ in the specificity function Eq. (4), enzymes replicate everything except their exact complement, because always $f_\mathrm{s}(L) = 0$).

From the bifurcation diagram obtained via Eq. (11), we easily read off exact results for the value $\tilde{\mu}_\mathrm{c} = \mu(1/2)$ where the delocalized state gains stability. E.g., for the generalized Schlögl model $p \to \infty$, we get $\tilde{\mu}_\mathrm{c} = \beta/(\alpha 2^{L+1} + 4\beta)$ (Stadler et al., 1995). This exponentially small yet finite value is consistent with our previous conclusion that the delocalized regime is stable for all values of $\mu$ within the error-tail approximation, Eq. (12), which holds for $L \to \infty$. Further, we find that the two critical values $\tilde{\mu}_\mathrm{c}$ and $\mu_\mathrm{c}$ are identical for $p = 0, 1, 2$. Recognizing that Fig. 2 describes a pitchfork bifurcation at $a = 1/2$ and $\mu = \tilde{\mu}_\mathrm{c}$, we infer that the two critical mutation rates are equal ($\mu_\mathrm{c} = \tilde{\mu}_\mathrm{c}$) whenever the pitchfork is supercritical, whereas bistability between localized and delocalized states for intermediate mutation rates $\tilde{\mu}_\mathrm{c} < \mu < \mu_\mathrm{c}$ is possible in the subcritical case, leading to the discontinuous transition observed in Fig. 1. The bistability regime vanishes as the curvature $\mu''(1/2)$ in the bifurcation diagram changes sign, which gives from Eq. (11) an approximate expression for the corresponding critical value of $\beta$:

$$\beta^* = \alpha \left[ \frac{S'^2(1/2)}{S''(1/2) - 2S'(1/2)} - S(1/2) \right]^{-1} . \tag{13}$$



Accepted manuscript

ACCEPTED MANUSCRIPT

This general result can readily be evaluated for any specificity function entering the auxiliary function $S(x)$ defined in Eq. (10). It predicts bistability for all values $\beta < \beta^* = \alpha\, 2^{L-1}(L-2)$ if $p \to \infty$ in our choice Eq. (4) of the specificity function, and no bistability for weak specificity because the critical value of the coupling constant is negative ($\beta^* \leq 0$) for small $p < p_{\min} = 2 + \mathcal{O}(L^{-1})$. Since the mean Hamming distance $\langle k \rangle = aL$ is discontinuous at the error threshold only in the bistability regime $\beta < \beta^*(p)$, we argue that the observation of a discontinuous mean replication rate (mean fitness) $\alpha + \beta S(1 - 2a(1-a))$ depends on the specificity of second order catalysis, which generalizes the result of Wagner et al. (2010).

The results of the binomial closure approximation Eq. (9) are summarized in the phase diagram Fig. 3, where the two critical mutation rates $\mu_c$ and $\tilde{\mu}_c$ are shown as functions of the selection strength $\beta$ and the specificity degree $p$ for $\alpha = 1$. The thick line denoted $\beta^*$ indicates the boundary of the bistability regime $\mu_c > \tilde{\mu}_c$. Fig. 2 demonstrates that the binomial approximation is quantitatively excellent in the supercritical situation $\beta > \beta^*$ (in particular, it gives exact results for $\mu_c$ and $\tilde{\mu}_c$), and qualitatively correct otherwise, where the values for $\mu_c$ are somewhat underestimated: near the error threshold, the variance of the population distribution is considerably larger than that of a binomial. Nevertheless, we emphasize that the result $\mu_c = \ln(\beta/\alpha)/(2L)$ in the limiting case $p \to \infty$ agrees with the value obtained from the error-tail approximation for large $\beta$. The remarkable performance of the binomial closure approximation can be appreciated in more detail from the projected phase diagrams shown in Fig. 4.

A noticeable feature of these phase diagrams is that the error threshold $\mu_c$ *increases* for stronger specificity $p$ (see Fig. 4(b)), which implies that higher mutation rates can be tolerated, i.e., that longer sequences can be maintained. This seems at first counter-intuitive, because weaker specificity constraints on the recognition sequence should allow more mutational "freedom". However, as shown in Fig. 2 and Fig. 1, smaller values for $p$ lead to much broader distributions: mutants are still reasonably well replicated by master enzymes, but the

Accepted manuscript

ACCEPTED MANUSCRIPT

master is only moderately well (but not quite as efficiently) replicated by the mutants. The resulting broadening of the distribution effectively reduces the replication rate of the master and escalates the error catastrophe (Obermayer and Frey, 2009). Thus, the necessity for an enzymatic replicator to discriminate not only between functional and non-functional *substrates*, but also between efficient and unproductive *enzymes*, is again emphasized.

We finally want to remark on the case $\alpha = 0$, i.e., no background level for the non-enzymatic replication rate. Most of the above results obtained from the binomial closure approximation can be simply evaluated for $\alpha = 0$ (note that then $\beta$ sets the timescale and drops out), but the strong specificity limit $p \to \infty$ deserves extra attention. The error-tail approximation indicates that the error threshold vanishes ($\mu_c \to 1$), but from Eq. (9) we find the *exact result* $\mu_c = \tilde{\mu}_c = 1/6$ for $L \gg 1$, i.e., a macroscopic yet finite value (see Appendix A.2). This remarkable result can be explained by recalling that the traditional result $\mu_c \approx \ln r/L$ (Eigen et al., 1989; Wiehe, 1997) for the error threshold depends on the replication advantage $r$ of the master relative to a possibly small but finite value for the mutants. In our case, rates are directly proportional to concentration, and because the master sequence has a concentration of order 1, while in an infinitely large population distant mutants have concentrations of order $2^{-L}$, this relative advantage itself is of order $2^L$, and cancels the length dependence of the error threshold. In the corresponding non-enzymatic case, results for so-called "truncation" fitness landscapes have lead to some debate about the applicability of the error threshold concept in the presence of lethal mutations (Wilke, 2005; Summers and Litwin, 2006; Takeuchi and Hogeweg, 2007; Saakian et al., 2009). Accordingly, we should cautiously note that our results for $\alpha = 0$ will probably be affected when accounting for the effects of finite populations and the full dependence of the replication rates on the genotypes of enzyme and substrate.

Accepted manuscript

ACCEPTED MANUSCRIPT

*4.2. Cross-specific replication*

To increase the information content of replicating systems beyond the limited complexity of a single replicator, auto-catalytic reaction networks such as hypercycles (Eigen and Schuster, 1978; Stadler et al., 1995) have been proposed, where different molecular species catalyze each other's replication in a possibly complex interaction graph. Only very little is known for these systems regarding the issue of reaction specificity and the cross-interactions of each species' mutant clouds. The simplest conceivable networks are 2-member cross-catalytic hypercycles. While the two members (which actually replicate via complementary intermediates) need not be strictly complementary, we assume that they are sufficiently distinct that an idealized model requiring complementary recognition regions captures the essentials. This suggests to analyze the specificity function Eq. (5) where replication rates increase with Hamming distance between enzyme and substrate. In this case, we expect the formation of two sub-populations localized about complementary sequences, each catalyzing the replication of the other. The main question to be answered is how specificity affects coexistence. In the standard Eigen model, quasispecies coexistence is prevented by competitive exclusion except in degenerate cases, because the "fittest" individuals take over the population (Swetina and Schuster, 1982). Interactions between sub-populations, e.g., based on complementarity of binary traits (de Oliveira and Fontanari, 2002), are known to enable coexistence. In our case, we expect novel conditions for coexistence: even though each subpopulation depends on the presence of the other for efficient replication, it is unclear how the possibly broad mutant distributions influence each other.

From numerical solutions to the reduced rate equations and simulation results, where we initialized the population split between the master sequence and its complement (see Fig. 5), we find that localization is only possible for $p > 1$. This important result is confirmed through the binomial moment closure approximation (see Appendix B.2), which has for $p = 1$ only the solution $a = 1/2$, corresponding to the delocalized state. Because the complementary distributions overlap too much if catalytic rates increase only linearly with Hamming



Accepted manuscript

ACCEPTED MANUSCRIPT

distance, the populations are not localized strongly enough to ensure coexistence.

The bifurcation diagram $\mu(a)$ obtained from our approximation scheme (see Eq. (B.7)) is shown in comparison with the exact result from the reduced rate equations in Fig. 6 for different values of $p$. We obtain information about the parameter $a$ from the variance $\langle \Delta k^2 \rangle = \sum_k (k - \langle k \rangle)^2 x_k$, in the case of two complementary binomials given by $\langle \Delta k^2 \rangle = L^2/4 - L(L-1)a(1-a)$. Using this expression to infer $a$ from the measured variance gives very good agreement between binomial closure approximation and exact numerical results especially for small $p$, because now the first *two* moments are correct. The critical mutation rates $\mu_c$ and $\tilde{\mu}_c$ can be found from the bifurcation diagram, e.g., $\mu_c = \mathcal{W}[\beta/(2\alpha e)]/(2L)$ for $p \to \infty$, which is identical to the corresponding result for self-specific replication if we replace $\beta \to \beta/2$. Hence, in this limit we obtain two clearly separated binomial distributions representing two equivalent and catalytically coupled populations: indeed, in the localized state the sum $x_k + x_{L-k}$ from Fig. 5(b) is equal to $x_k$ in the self-specific situation shown in Fig. 1(c) once we replace $\beta \to \beta/2$. The "coupling constant" is only half as large because only one half of the population is available as enzymes for the other. In particular, the negligible interaction between the respective mutant clouds allows one to employ the error-tail approximation assuming independent species and error tails as in (Campos et al., 2000; Obermayer and Frey, 2009). Further, we find that the pitchfork bifurcation is always subcritical, i.e., that $\mu_c > \tilde{\mu}_c$. We summarize our main results by plotting projected phase diagrams of $\mu_c$ and $\tilde{\mu}_c$ as functions of $p-1$ and $\beta$ in Fig. 7. This confirms that both critical mutation rates $\mu_c$ and $\tilde{\mu}_c$ vanish linearly with $p-1$, because $\mu(a) \propto p-1$ as $p \to 1$, which gives the sharp bound $p > 1$ for coexistence of two populations. Finally, the case $\alpha = 0$ of zero non-enzymatic replication rate is similar to the self-specific case: the slight chance of distant mutants to find an appropriate enzyme gives an enormous replication advantage to the mainly populated master sequences and therefore macroscopic values for the error threshold (see Appendix B.3 for details).



Accepted manuscript

ACCEPTED MANUSCRIPT

## 5. Conclusion

Because enzymatic replication provokes the necessity for enzymes to favor functional substrates and for substrates to prefer efficient enzymes, we analyzed the effects of specific replication on the error threshold. In our model, which accounts for the full quasispecies mutant distributions, replication rates depend on the Hamming distance between enzyme and substrate via an adjustable degree of specificity. Combining stochastic simulations, numerical solutions of reduced rate equations and analytical solutions to a binomial closure approximation, we could analyze the entire phase diagram and assess how mutation rate $\mu$, selection strength $\beta$ and specificity degree $p$ influence the localization about a master sequence in order to preserve its information content. We found that for self-specific replication very weak specificity suffices for localization, whereas stronger specificity gives more tolerance against mutations but leads to bistability with the delocalized regime of random sequences. In particular, the binomial closure approximation permits to obtain analytical expressions for the bifurcation diagram and an upper bound $\beta^*$ for the bistability regime, which can be evaluated for any specificity function $f_{\mathrm{s}}(d)$. Apart from our special choice, Eq. (4), a mesa-shaped function would also be conceivable, in correspondence to fitness landscapes for transcription factor binding allowing for some "fuzziness" or neutrality in the binding sequence (Gerland and Hwa, 2002). Preliminary results indicate that in this case the binomial closure approximation gives at least qualitative agreement as well. While our approximation is not restricted to large $L$, this limit can probably be more systematically be described using the maximum principle employed previously in quasispecies theory (Hermisson et al., 2002; Saakian and Hu, 2006). In the case of cross-specificity, we found that coexistence of subpopulations localized about complementary sequences is possible only if replication rates increase faster than linearly with Hamming distance.

Although our model is based on idealizing assumptions, we can extrapolate from currently available experimental data to obtain rough quantitative esti-

Accepted manuscript

ACCEPTED MANUSCRIPT

mates for the maximal length $L_c$ of the recognition or tag sequences that can be used by replicase enzymes to specifically and reliably discriminate appropriate and useless templates (and vice versa). Considering that non-enzymatic template-directed polymerization rates are on the order of several hours to days per base (Acevedo and Orgel, 1987; Wu and Orgel, 1992), while ribozyme-catalyzed polymerization gives rates in the hour range (Johnston et al., 2001; Zaher and Unrau, 2007), we can estimate the ratio $\beta/\alpha$ somewhere near 5-20 if polymerization is the rate-limiting step. Assuming a self-specific enzymatic replicator with a mutation rate on the order of 3% as in (Johnston et al., 2001), we obtain a critical length $L_c$ = 11-15 for weak specificity $p = 1$, and a larger value $L_c$ = 18-33 for $p \to \infty$, because stronger specificity constraints allow longer sequences due to better localization. These values are significantly smaller than the lengths of, e.g., the 154-nucleotide specificity domain of *Bacillus subtilis* RNase P (Lilley, 2005) or the tRNA-like structures supposed to act as "genomic tags" for the replication of RNA viruses (Weiner and Maizels, 1987). Many of the nucleotides in these instances have a structural role, which makes them effectively redundant or neutral (Kun et al., 2005), and only a minority is actually involved in recognition. Also, recent research indicates that "stalling" of polymerization after mismatch incorporation might significantly reduce the error threshold (Rajamani et al., 2010). Nevertheless, our result suggests that the error threshold puts hard constraints on the information content of enzymatic replicators as well.

Accepted manuscript

**Acknowledgements**

We gratefully acknowledge helpful discussions with Joachim Krug and Irene Chen and financial support by the German Excellence Initiative via the program "Nanosystems Initiative Munich" and by the Deutsche Forschungsgemeinschaft through SFB TR12.

ACCEPTED MANUSCRIPT

Figure 1: Solutions for self-specific replication with $f_{\mathrm{s}}(d) = (1 - d/L)^p$. Stationary Hamming distance distribution $x_k$ as function of mutation rate $\mu$ from numerical solutions to the reduced rate equations Eq. (6) (straight lines) and a stochastic simulation of the full system Eq. (1) in a population of $N = 10^4$ sequences of length $L = 32$ (dots) for $\alpha = 1$, $\beta = 5$ and (a) $p = 1$, (b) $p = 5$, and (c) $p = \infty$ (here, the dashed line shows the error-tail approximation for $x_0$). The insets depict the average Hamming distance $a = \langle k \rangle / L$ to the master sequence.

Figure 2: Bifurcation diagram of Eq. (6) for the normalized mean Hamming distance $a = \langle k \rangle / L$ with $L = 8$, $\alpha = 1$, $\beta = 1$ and different values of the specificity degree $p$. Thick lines indicate stable branches, dashed lines unstable branches and thin dotted lines the results of the binomial closure approximation Eq. (9), which is barely visible for $p = 0.1$ and $p = 1$. Circles indicate critical mutation rates $\mu_{\mathrm{c}}$ where the localized regime vanishes, crosses show values $\tilde{\mu}_{\mathrm{c}}$ where the delocalized state changes stability (horizontal branches corresponding to delocalized states are drawn slightly shifted for visualization).

Figure 3: Phase diagram of localization regimes in the parameter space of mutation rate $\mu$, selection strength $\beta$ and specificity degree $p$ (log-log-log scale) obtained from Eq. (9) for $L = 8$ and $\alpha = 1$: below the upper plane $\mu_{\mathrm{c}}$, a localized solution exists, while above the lower plane $\tilde{\mu}_{\mathrm{c}}$ the delocalized state becomes stable. Bistability ($\mu_{\mathrm{c}} > \tilde{\mu}_{\mathrm{c}}$) is possible only for $\beta < \beta^*(p)$.

Figure 4: Projected phase diagrams of localization regimes for self-specific replication with $L = 8$ and $\alpha = 1$ obtained from Eq. (6): (a) as function of $\beta$ with $p = 10$ fixed; (b) as function of $p$ with $\beta = 10$ fixed. Below $\mu_{\mathrm{c}}$ (thick line), a localized solution exists, while above $\tilde{\mu}_{\mathrm{c}}$ (thick dashed line) the delocalized state becomes stable. The dotted lines denote the result for $\mu_{\mathrm{c}}$ obtained via the binomial closure approximation. Bistability ($\mu_{\mathrm{c}} > \tilde{\mu}_{\mathrm{c}}$) is possible only for $\beta < \beta^*(p)$ (or $p > p^*(\beta)$).

Figure 5: Hamming distance distribution $x_k$ as function of mutation rate $\mu$ as in Fig. 1, but for cross-specific replication with $\alpha = 1$, $\beta = 10$, $L = 32$, and (a) $p = 5$ or (b) $p = \infty$. The insets show the variance $\langle \Delta k^2 \rangle = \sum_k (k - \langle k \rangle)^2 x_k$ (in a symmetric population, $\langle k \rangle = L/2$).

Figure 6: Bifurcation diagram of Eq. (6) as in Fig. 2, but for cross-specific replication in terms of the population parameter $a$, which denotes the width of the two subpopulations and is calculated from the variance $\langle \Delta k^2 \rangle$ in the Hamming distance distribution. Parameters are $L = 8$, $\alpha = 1$, and $\beta = 1$.

Figure 7: Projected phase diagrams of localization regimes as in Fig. 4, but for cross-specific replication with $L = 8$ and $\alpha = 1$: (a) as function of $\beta$ with $p = 10$ fixed; (b) as function of $p$ with $\beta = 10$ fixed.

Accepted manuscript

ACCEPTED MANUSCRIPT

## Appendix A. Self-specific replication

*Appendix A.1. Derivation of Eq.* (9)

To obtain Eq. (9), we compute the first moment $\sum_k k\dot{x}_k$ of the reduced rate equations Eq. (6) under the assumption that $x_k = x_k^{\mathrm{b}} \equiv \binom{L}{k} a^k (1-a)^{L-k}$ is binomially distributed. This gives four terms

$$\begin{aligned} T_1 &= \sum_{jk} k\, m_{kj} a_j x_j^{\mathrm{b}} & T_2 &= \sum_{ijk} k\, m_{kj} b_{ji} x_i^{\mathrm{b}} x_j^{\mathrm{b}} \\ T_3 &= -\sum_k k\, x_k^{\mathrm{b}} \sum_j a_j x_j^{\mathrm{b}} & T_4 &= -\sum_k k\, x_k^{\mathrm{b}} \sum_{ij} b_{ji} x_i^{\mathrm{b}} x_j^{\mathrm{b}}. \end{aligned} \tag{A.1}$$

The reduced mutation matrix $m_{kj}$ and the catalytic matrix $b_{ij}$ are given in Eqs. (7) and (8). Note that although not immediately obvious, the catalytic matrix $b_{ij} = b_{ji}$ is symmetric, because the binomial in the denominator of Eq. (8) normalizes it to the single sequence level. We further keep in mind that $\binom{n}{k} = 0$ if $k < 0$ or $k > n$ if $n$ and $k$ are integer, so we do not need to keep track of the summation limits in the following calculations.

While it is straightforward to find $T_1 = \alpha L(a + \mu(1-2a))$ and $T_3 = -\alpha a L$, we concentrate first on $T_4$, which reads after performing the summation over $k$

$$T_4 = -\beta a L \sum_{ijn} \binom{L-j}{i-j+n} \binom{L}{j} \binom{j}{n} f_{\mathrm{s}}(i-j+2n) a^{i+j} (1-a)^{2L-(i+j)}. \tag{A.2}$$

Replacing $i' = i - j + 2n$ and rearranging $\binom{L-j}{i'-n}\binom{L}{j}\binom{j}{n} = \binom{L-i'}{j-n}\binom{L}{i'}\binom{i'}{n}$, we can sum over $j$ and $n$, and are left with

$$\begin{aligned} T_4 &= -\beta a L \sum_{i'} \binom{L}{i'} f_{\mathrm{s}}(i') (1 - 2a(1-a))^{L-i'} (2a(1-a))^{i'} \\ &= -\beta a L S (1 - 2a(1-a)). \end{aligned} \tag{A.3}$$

The term $T_2$ can after similar rearrangements be written as the product of two generalized Vandermonde matrices:

$$T_2 = \beta \sum_{i'} \binom{L}{i'} f_{\mathrm{s}}(i') \sum_{jk} k \begin{bmatrix} \mu & 1-\mu \\ 1-\mu & \mu \end{bmatrix}_{L-k,j} \begin{bmatrix} (1-a)^2 & a(1-a) \\ a^2 & a(1-a) \end{bmatrix}_{j,i}, \tag{A.4}$$

ACCEPTED MANUSCRIPT

where the $L^{\text{th}}$ Vandermonde matrix with parameters $a$, $b$, $c$, and $d$ is defined as

$$\begin{bmatrix} a & b \\ c & d \end{bmatrix}_{i,j} \equiv \sum_{\ell} \binom{L-j}{i-\ell}\binom{j}{\ell} a^{L+\ell-i-j} b^{j-\ell} c^{i-\ell} d^{\ell}. \tag{A.5}$$

This allows us to use a nice multiplication identity (Rawlings and Sze, 2005) for these matrices:

$$\begin{bmatrix} a & b \\ c & d \end{bmatrix} \begin{bmatrix} e & f \\ g & h \end{bmatrix} = \begin{bmatrix} ae+bg & af+bh \\ ce+dg & cf+dh \end{bmatrix}, \tag{A.6}$$

which gives:

$$T_2 = \beta \sum_{i'} \binom{L}{i'} f_{\mathrm{s}}(i') \sum_{k} k \begin{bmatrix} a^2+\mu(1-2a) & a(1-a) \\ (1-a)^2-\mu(1-2a) & a(1-a) \end{bmatrix}_{L-k,i'} \tag{A.7}$$

$$= \beta\big[L(a+\mu(1-2a))S(1-2a(1-a)) \tag{A.8}$$

$$- (1-2a)a(1-a)(1-2\mu)S'(1-2a(1-a))\big]. \tag{A.9}$$

Adding up $T_1+T_2+T_3+T_4=0$ gives Eq. (9).

*Appendix A.2. Solutions of Eq.* (9)

This equation can be solved whenever $S(x)$, defined in Eq. (10), assumes a simple form. For $f_{\mathrm{s}}(d) = (1-d/L)^p$ as in Eq. (4), $S(x)$ is a polynomial of order $L$, except for integer $0 < p < L$, where it is of order $p$. A few instances for $L > 2$ are given by

$$S(x) = \begin{cases} 1-(1-x)^L, & p=0, \\ x, & p=1, \\ \frac{1}{L}x + \frac{L-1}{L}x^2, & p=2, \\ x^L, & p=\infty. \end{cases} \tag{A.10}$$

To find solutions $a(\mu) \neq 1/2$, we write $x = a(1-a)$ and solve Eq. (9) for $x$:

$$x = \begin{cases} \frac{1}{2}\left(2\mu\frac{\alpha+\beta}{\beta}\right)^{1/L}, & p=0 \\ \frac{\alpha+\beta}{\beta}\frac{\mu L}{1+2\mu(L-1)}, & p=1 \\ \mu - \frac{1}{2L}\mathcal{W}\left(-\frac{2\alpha\mu L}{\beta}\mathrm{e}^{2\mu L}\right), & p=\infty. \end{cases} \tag{A.11}$$



Accepted manuscript

ACCEPTED MANUSCRIPT

For the last case, we approximated $(1-2x)^L \approx \mathrm{e}^{-2xL}$ and $\mu/(1-2\mu) \approx \mu$ for the important asymptote $L \gg 1$ with $\mu L$ fixed, and used Lambert's $\mathcal{W}$-function. A more complicated expression is obtained for $p = 2$. The solution $a = \frac{1}{2}\left(1 \pm \sqrt{1-4x}\right)$ is then easily computed, and the error thresholds $\mu_\mathrm{c}$ follow from evaluating the condition $x = 1/4$ (for $p = 0, 1, 2$), or from requiring the $\mathcal{W}$-function to give a real result (for $p = \infty$):

$$\mu_\mathrm{c} = \begin{cases} \frac{\beta}{\alpha+\beta} 2^{-(L+1)}, & p = 0, \\ \frac{\beta}{4\alpha L + 2\beta(L+1)}, & p = 1, \\ \frac{\beta}{4\alpha L + \beta(L+3)}, & p = 2, \\ \frac{1}{2L}\mathcal{W}\left(\frac{\beta}{\mathrm{e}\alpha}\right), & p = \infty. \end{cases} \tag{A.12}$$

Finally, it is easy to evaluate the bifurcation diagram Eq. (11) at $a = 1/2$ to get the critical mutation rate $\tilde{\mu}_\mathrm{c} = \mu(1/2)$:

$$\tilde{\mu}_\mathrm{c} = \frac{\beta S'(1/2)}{2\beta S'(1/2) + 4L(\alpha + \beta S(1/2))}. \tag{A.13}$$

For our specificity function $f_\mathrm{s}(d) = (1-d/L)^p$, we obtain explicitly

$$\tilde{\mu}_\mathrm{c} = \begin{cases} 2^{-(L+1)} \frac{\beta}{\alpha+\beta}, & p = 0 \\ \frac{\beta}{4\alpha L + 2\beta(L+1)}, & p = 1 \\ \frac{\beta}{4\alpha L + \beta(L+3)}, & p = 2 \\ \frac{\beta}{\alpha 2^{L+1} + 4\beta}, & p = \infty. \end{cases} \tag{A.14}$$

Note that $\mu_\mathrm{c} = \tilde{\mu}_\mathrm{c}$ for $p \leq 2$.

While most of these results can be evaluated also for $\alpha = 0$, the case $p \to \infty$ is special. Here, Eq. (9) gives $x = \mu/(1-2\mu)$ if we again approximate $(1-2x)^L \approx \mathrm{e}^{-2xL}$, hence the error threshold is $\mu_\mathrm{c} = 1/6$, independent of $\beta$ and $L$.

## Appendix B. Cross-specific replication

### *Appendix B.1. Derivation of an equation for a*

To obtain an equation for the parameter $a$, we compute the second moment $\sum_k k^2 \dot{x}_k$ of the reduced rate equations, Eq. (6), under the assumption that



Accepted manuscript

ACCEPTED MANUSCRIPT

$x_k = x_k^{\mathrm{c}} \equiv \frac{1}{2}\binom{L}{k}[a^k(1-a)^{L-k} + a^{L-k}(1-a)^k]$ is a sum of two complementary binomials, because in this case the first moment vanishes by construction. The four terms $T_1$-$T_4$ are defined and evaluated analogously to Eq. (A.1), and after some algebra we find:

$$T_1 = \frac{1}{2}\alpha L\left[L - 2(L-1)(a(1-a)(1-2\mu)^2 + \mu(1-\mu))\right] \tag{B.1}$$

$$\begin{aligned} T_2 = \frac{1}{2}\beta\Big[&L(L-2(L-1)(a+\mu(1-2a))(1-a-\mu(1-2a)))C(1-2a(1-a)) \\ &+ 2a(1-a)(1-2a)^2(1-2\mu)^2(L-1)C'(1-2a(1-a)) \\ &+ 2(a(1-a)(1-2a)(1-2\mu))^2C''(1-2a(1-a))\Big] \end{aligned} \tag{B.2}$$

$$T_3 = -\frac{1}{2}\alpha L[L-2(L-1)a(1-a)] \tag{B.3}$$

$$T_4 = -\frac{1}{2}\beta L[L-2(L-1)a(1-a)]C(1-2a(1-a)). \tag{B.4}$$

Here, we have defined $C(x) = \frac{1}{2}\sum_k \binom{L}{k}\left[f_{\mathrm{c}}(k) + f_{\mathrm{c}}(L-k)\right]x^{L-k}(1-x)^k$. Adding up $T_1 + T_2 + T_3 + T_4 = 0$ gives the condition

$$\begin{aligned} (1-2a)^2\Big\{&\mu(1-\mu)L(L-1)\big[\alpha + \beta C(1-2a(1-a))\big] \\ &- \beta a(1-a)(1-2\mu)^2\big[(L-1)C'(1-2a(1-a)) \\ &+ a(1-a)C''(1-2a(1-a))\big]\Big\} = 0. \end{aligned} \tag{B.5}$$

Most importantly, Eq. (B.5) reads for $p = 1$ in the specificity function $f_{\mathrm{c}}(d) = (d/L)^p$:

$$-(1-2a)^2L(L-1)\mu(1-\mu)(\alpha + \beta/2) = 0, \tag{B.6}$$

which has only the solution $a = 1/2$.

*Appendix B.2. Bifurcation diagram*

Solving Eq. (B.5) for $\mu$ gives the bifurcation diagram:

$$\mu(a) = \frac{1}{2}\left[1 \pm \left(1 + \frac{4\beta a(1-a)\big[(L-1)C'(1-2a(1-a)) + a(1-a)C''(1-2a(1-a))\big]}{L(L-1)[\alpha+\beta C(1-2a(1-a))]}\right)^{-1/2}\right], \tag{B.7}$$



Accepted manuscript

ACCEPTED MANUSCRIPT

where we take the negative sign and the positive root to obtain values $\mu$ near zero (values near unity imply complementary replication and give equivalent results for cross-specific replication).

We readily find that $\mu''(1/2) > 0$ if $\beta > 0$, which implies that the pitchfork bifurcation described through Eq. (B.7) is always subcritical.

*Appendix B.3. Solutions of Eq.* (B.5)

The auxiliary function $C(x)$ can be evaluated for small integer $p$ as in Eq. (A.10). There is no solution to Eq. (B.5) except $a = 1/2$ for $p = 1$, and the expression for $p = 2$ is quite lengthy. For $p = \infty$ and $\alpha > 0$, we get

$$x = a(1-a) = \mu - \frac{1}{2L}\mathcal{W}\left(\frac{4\alpha\mu L}{\beta}\mathrm{e}^{2\mu L}\right), \tag{B.8}$$

which is exactly the result for the self-specific case if we replace $\beta \to \beta/2$. Accordingly, we get $\mu_\mathrm{c} = \mathcal{W}[\beta/(2\mathrm{e}\alpha)]/(2L)$ for the error threshold.

Observing that $C'(1/2) = 0$, the critical mutation rate $\tilde{\mu}_\mathrm{c} = \mu(1/2)$ is given by

$$\tilde{\mu}_\mathrm{c} = \frac{1}{2}\left[1 - \left(1 + \frac{\beta C''(1/2)}{4L(L-1)(\alpha + \beta C(1/2))}\right)^{-1/2}\right], \tag{B.9}$$

which reads explicitly

$$\tilde{\mu}_\mathrm{c} = \begin{cases} 0, & p = 1 \\ \frac{1}{2}\left[1 - \left(1 + \frac{2\beta}{4\alpha L^2 + \beta L(L+1)}\right)^{-1/2}\right], & p = 2 \\ \frac{1}{2}\left[1 - \left(1 + \frac{\beta}{\alpha 2^L + \beta}\right)^{-1/2}\right], & p = \infty. \end{cases} \tag{B.10}$$

We can simply take $\alpha = 0$ in most of the above expressions to investigate the case of zero non-enzymatic replication rate. In the limits $p \to \infty$ and $L \to \infty$, we find that the bifurcation diagram $\mu(a)$ converges towards

$$\mu(a) \to a(1-a), \tag{B.11}$$

except for a region near $a = 1/2$, because $\mu(1/2)$ has to coincide with the exact value $\tilde{\mu}_\mathrm{c} = (2 - \sqrt{2})/4$. Because this region becomes infinitesimally small as $L \to \infty$, we conclude that $\mu_\mathrm{c} \to 1/4$ in this limit.



Accepted manuscript

ACCEPTED MANUSCRIPT

## References

Acevedo, O.L., Orgel, L.E., 1987. Non-enzymatic transcription of an oligodeoxynucleotide 14 residues long. J. Mol. Biol. 197, 187–93.

Alves, D., Campos, P.R.A., Silva, A.T.C., Fontanari, J.F., 2001. Group selection models in prebiotic evolution. Phys. Rev. E 63, 011911.

Baake, E., Wiehe, T., 1997. Bifurcations in haploid and diploid sequence space models. J. Math. Biol. 35, 321–343.

Blythe, R.A., 2009. Generic modes of consensus formation in stochastic language dynamics. J. Stat. Mech.-Theory Exp. , P02059.

Campos, P.R.A., Fontanari, J.F., Stadler, P.F., 2000. Error propagation in the hypercycle. Phys. Rev. E 61, 2996–3002.

Cech, T.R., 1990. Nobel lecture. Self-splicing and enzymatic activity of an intervening sequence RNA from *tetrahymena*. Biosci. Rep. 10, 239–61.

Doudna, J., Cech, T., 2002. The chemical repertoire of natural ribozymes. Nature 418, 222–228.

Eigen, M., McCaskill, J., Schuster, P., 1989. The molecular quasi-species. Adv. Chem. Phys. 75, 149–263.

Eigen, M., Schuster, P., 1978. The hypercycle – a principle of natural self-organization. Part B: The abstract hypercycle. Naturwissenschaften 65, 7–41.

Fernando, C., von Kiedrowski, G., Szathmáry, E., 2007. A stochastic model of nonenzymatic nucleic acid replication: "elongators" sequester replicators. J. Mol. Evol. 64, 572–585.

Fontanari, J.F., Santos, M., Szathmáry, E., 2006. Coexistence and error propagation in pre-biotic vesicle models: A group selection approach. J. Theor. Biol. 239, 247–256.

Accepted manuscript

ACCEPTED MANUSCRIPT

Galluccio, S., 1997. Exact solution of the quasispecies model in a sharply peaked fitness landscape. Phys. Rev. E 56, 4526–4539.

Gerland, U., Hwa, T., 2002. On the selection and evolution of regulatory DNA motifs. J. Mol. Evol. 55, 386–400.

Gilbert, W., 1986. Origin of life – the RNA world. Nature 319, 618–618.

Hermisson, J., Redner, O., Wagner, H., Baake, E., 2002. Mutation-selection balance: Ancestry, load, and maximum principle. Theor. Popul. Biol. 62, 9–46.

Huynen, M.A., Stadler, P., Fontana, W., 1996. Smoothness within ruggedness: The role of neutrality in adaptation. Proc. Natl. Acad. Sci. U.S.A. 93, 397–401.

Jain, K., Krug, J., 2005. Adaptation in simple and complex fitness landscapes. arXiv: q-bio/0508008.

Johnston, W.K., Unrau, P.J., Lawrence, M.S., Glasner, M.E., Bartel, D.P., 2001. RNA-catalyzed RNA polymerization: accurate and general RNA-templated primer extension. Science 292, 1319–25.

Joyce, G.F., 2007. Forty years of in vitro evolution. Angew. Chem. Int. Ed. 46, 6420–36.

von Kiedrowski, G., 1986. A self-replicating hexadeoxynucleotide. Angew. Chem. Int. Ed. 25, 932–935.

Komarova, N.L., 2004. Replicator-mutator equation, universality property and population dynamics of learning. J. Theor. Biol. 230, 227–239.

Kun, A., Santos, M., Szathmáry, E., 2005. Real ribozymes suggest a relaxed error threshold. Nat. Genet. 37, 1008–1011.

Lässig, M., Tria, F., Peliti, L., 2003. Evolutionary games and quasispecies. Europhys. Lett. 62, 446–451.

Accepted manuscript

ACCEPTED MANUSCRIPT

Leuthäusser, I., 1986. An exact correspondence between Eigen's evolution model and a two-dimensional Ising system. J. Chem. Phys. 84, 1884–1885.

Lilley, D.M.J., 2005. Structure, folding and mechanisms of ribozymes. Curr. Opin. Struc. Biol. 15, 313–23.

Lincoln, T., Joyce, G.F., 2009. Self-sustained replication of an RNA enzyme. Science 323, 1229–1232.

Maynard Smith, J., 1979. Hypercycles and the origin of life. Nature 280, 445–446.

Michod, R.E., 1983. Population biology of the first replicators - on the origin of the genotype, phenotype and organism. Am. Zool. 23, 5–14.

Nowak, M.A., Komarova, N.L., Niyogi, P., 2001. Evolution of universal grammar. Science 291, 114–118.

Obermayer, B., Frey, E., 2009. Escalation of error catastrophe for enzymatic self-replicators. Europhys. Lett. 88, 48006.

de Oliveira, V.M., Fontanari, J.F., 2002. Complementarity and diversity in a soluble model ecosystem. Phys. Rev. Lett. 89, 148101.

Orgel, L.E., 1992. Molecular replication. Nature 358, 203–209.

Orgel, L.E., 2004. Prebiotic chemistry and the origin of the RNA world. Crit. Rev. Biochem. Mol. 39, 99–123.

Pace, N.R., Marsh, T.L., 1985. RNA catalysis and the origin of life. Orig. Life Evol. Biosphere 16, 97–116.

Peliti, L., 2002. Quasispecies evolution in general mean-field landscapes. Europhys. Lett. 57, 745–751.

Rajamani, S., Ichida, J.K., Antal, T., Treco, D.A., Leu, K., Nowak, M.A., Szostak, J.W., Chen, I.A., 2010. Effect of stalling after mismatches on the

Accepted manuscript

ACCEPTED MANUSCRIPT

error catastrophe in nonenzymatic nucleic acid replication. J. Am. Chem. Soc. 132, 5880–5885.

Rawlings, D., Sze, L., 2005. On the metamorphosis of vandermonde's identity. Mathematics Magazine 78, 232–238.

Saakian, D.B., Biebricher, C.K., Hu, C.K., 2009. Phase diagram for the Eigen quasispecies theory with a truncated fitness landscape. Phys. Rev. E 79, 041905.

Saakian, D.B., Hu, C.K., 2006. Exact solution of the Eigen model with general fitness functions and degradation rates. Proc. Natl. Acad. Sci. U.S.A. 103, 4935–4939.

Schuster, P., Swetina, J., 1988. Stationary mutant distributions and evolutionary optimization. Bull. Math. Biol. 50, 635–660.

Stadler, P.F., 1991. Complementary replication. Math. Biosci. 107, 83–109.

Stadler, P.F., Schnabl, W., Forst, C.V., Schuster, P., 1995. Dynamics of small autocatalytic reaction networks. 2. Replication, mutation and catalysis. Bull. Math. Biol. 57, 21–61.

Summers, J., Litwin, S., 2006. Examining the theory of error catastrophe. J. Virol. 80, 20–26.

Swetina, J., Schuster, P., 1982. Self-replication with errors – a model for polynucleotide replication. Biophys. Chem. 16, 329–345.

Szathmáry, E., Demeter, L., 1987. Group selection of early replicators and the origin of life. J. Theor. Biol. 128, 463–486.

Szostak, J.W., Bartel, D.P., Luisi, P.L., 2001. Synthesizing life. Nature 409, 387–309.

Takeuchi, N., Hogeweg, P., 2007. Error-threshold exists in fitness landscapes with lethal mutants. BMC Evol. Biol. 7, 15.

Accepted manuscript

ACCEPTED MANUSCRIPT

Takeuchi, N., Poorthuis, P., Hogeweg, P., 2005. Phenotypic error threshold; additivity and epistasis in RNA evolution. BMC Evol. Biol. 5, 9.

Wagner, N., Tannenbaum, E., Ashkenasy, G., 2010. Second order catalytic quasispecies yields discontinuous mean fitness at error threshold. Phys. Rev. Lett. 104, 188101.

Weiner, A.M., Maizels, N., 1987. Transfer RNA-like structures tag the 3' ends of genomic RNA molecules for replication – implications for the origin of protein-synthesis. Proc. Natl. Acad. Sci. U.S.A. 84, 7383–7387.

Wiehe, T., 1997. Model dependency of error thresholds: the role of fitness functions and contrasts between the finite and infinite sites models. Genet. Res. 69, 127–136.

Wilke, C.O., 2005. Quasispecies theory in the context of population genetics. BMC Evol. Biol. 5, 44.

Wilke, C.O., Ronnewinkel, C., Martinetz, T., 2001. Dynamic fitness landscapes in molecular evolution. Phys. Rep. 349, 395–446.

Woodcock, G., Higgs, P.G., 1996. Population evolution on a multiplicative single-peak fitness landscape. J. Theor. Biol. 179, 61–73.

Wu, T.F., Orgel, L.E., 1992. Nonenzymatic template-directed synthesis on oligodeoxycytidylate sequences in hairpin oligonucleotides. J. Am. Chem. Soc. 114, 317–322.

Zaher, H.S., Unrau, P.J., 2007. Selection of an improved RNA polymerase ribozyme with superior extension and fidelity. RNA 13, 1017–1026.

Accepted manuscript

ACCEPTED MANUSCRIPT

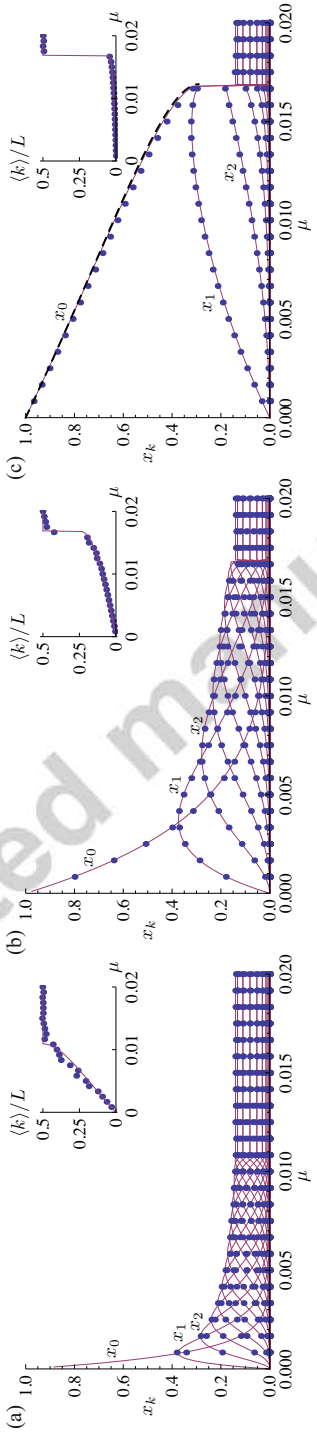


Accepted manuscript

ACCEPTED MANUSCRIPT

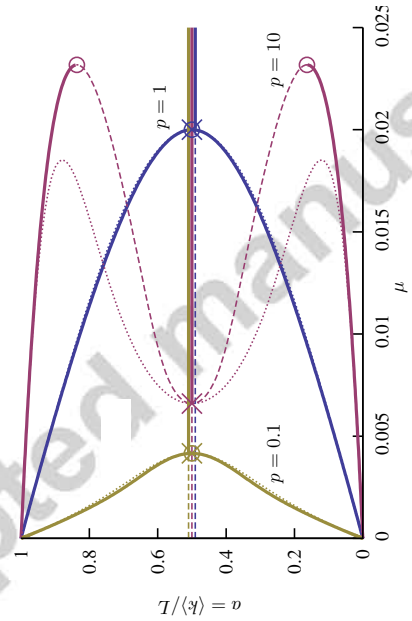


Accepted manuscript

ACCEPTED MANUSCRIPT

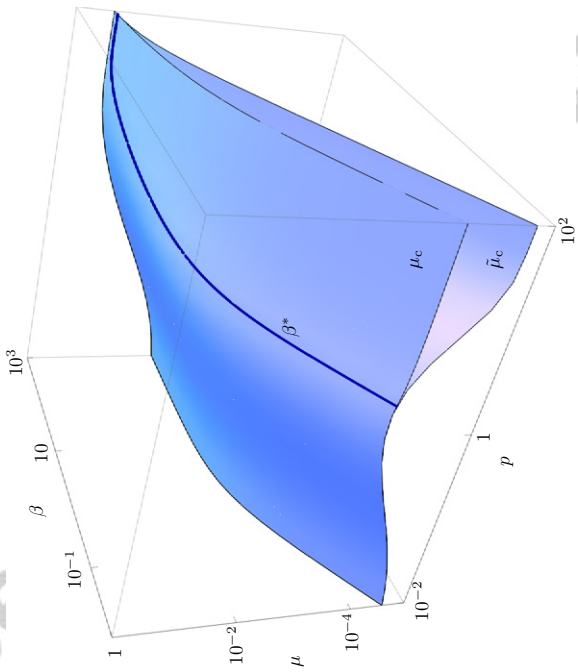

ACCEPTED MANUSCRIPT

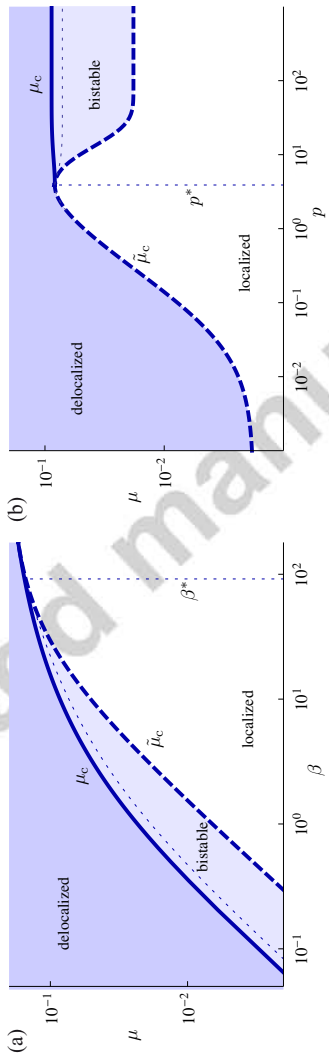


Accepted manuscript

ACCEPTED MANUSCRIPT

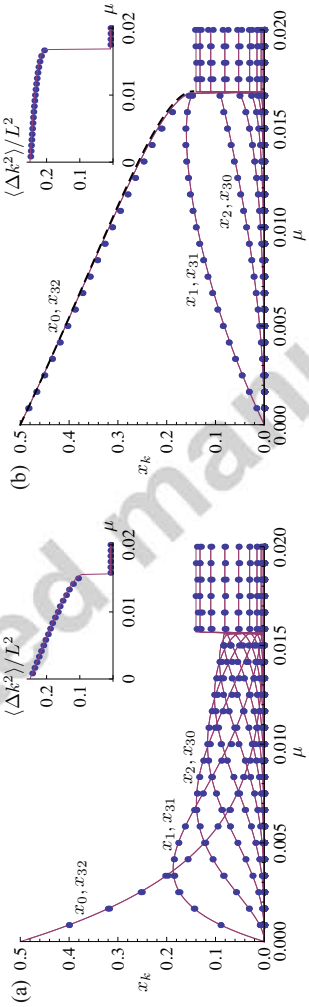


Accepted manuscript

ACCEPTED MANUSCRIPT

## 4. Figure

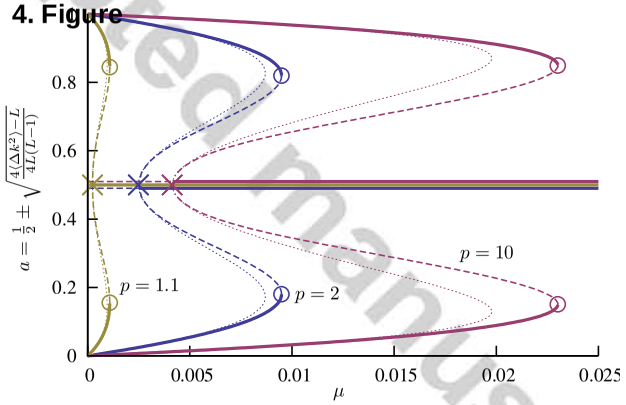


Accepted manuscript

ACCEPTED MANUSCRIPT

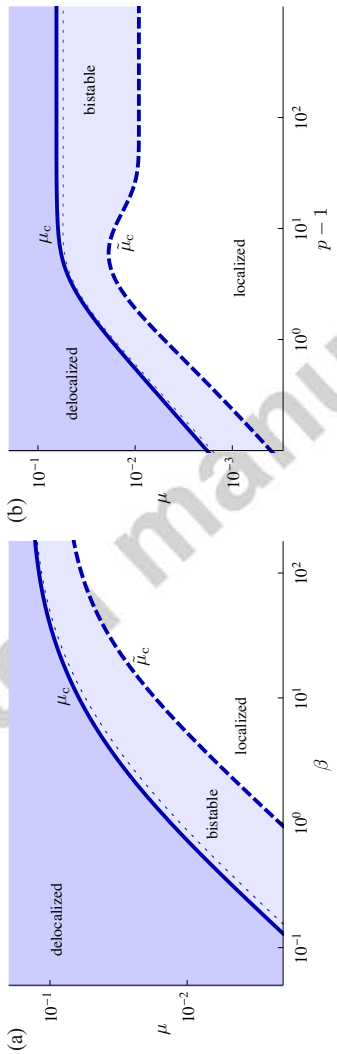


Accepted manuscript